Accelerated Publications

High-Risk HPV E6 Oncoproteins Assemble into Large Oligomers that Allow Localization of Endogenous Species in Prototypic HPV-Transformed Cell Lines†

María M. García-Alai,‡ Karina I. Dantur,‡ Clara Smal,‡ Lía Pietrasanta,§ and Gonzalo de Prat-Gay*,‡

Instituto Leloir and CONICET, Patricias Argentinas 435, 1405 Buenos Aires, Argentina, and Facultad de Ciencias Exactas y Naturales, UBA, Buenos Aires, Argentina

Received November 29, 2006

ABSTRACT: The E6 oncoproteins of high-risk HPV types 16 and 18 are involved in the development of cervical cancer. Besides its determinant role in carcinogenic progression, HPV E6 oncoprotein has also been instrumental in elucidating fundamental aspects of p53 function and its ubiquitin−proteasome degradation, with counterpart activities in various DNA tumor viruses. Establishing the conformational state and cellular distribution unequivocally for the endogenous protein in HPV-transformed cell lines derived from carcinomas is essential for understanding the underlying mechanism. Recombinant E6 from high-risk strains 16 and 18 folds into soluble oligomers of ∼1.2 MDa, which are thermostable and display cooperative loss of tertiary and secondary structure upon chemical denaturation. Antibodies raised against these assemblies locate E6 evenly distributed in the cells. By depleting the polyclonal serum by immunoblocking with monomeric E6, the nuclei of Hela and CaSki cells become completely devoid of label, indicating that monomeric species are mainly localized in the nucleus and that both monomers and oligomers share epitopes. The monomeric species promote degradation of p53 by the proteasome, which correlates with the nuclear localization we describe. In contrast, the oligomeric E6 does not promote p53 degradation, in agreement with its cytoplasmic localization inferred from the immunoneutralization experiments. Our results indicate that the cytoplasmic species contain conformational epitopes that may arise from yet undefined homo or hetero-oligomers, but its localization otherwise agrees with that of the other group of major E6 targets, those involving PDZ binding domains, which requires further investigation.

The determination of the molecular mechanisms through which human papillomaviruses (HPV) transform cells and promote malignant invasion is essential for understanding the development of cervical cancer, a major worldwide threat, and other types of neoplasic diseases linked to these viruses (*1*, *2*). In addition, HPV oncoproteins, as well as other DNA tumor virus counterparts, have been and continue to be essential in uncovering fundamental molecular aspects of both carcinogenesis and basic processes such as cell cycle control and proteasomal degradation of proteins (*3*, *4*).

There are more than 100 types of papillomaviruses, all with the potential to infect squamous epithelia (*5*). Low-risk mucosal human papillomaviruses such as HPV6 and HPV11 cause genital warts, while high-risk HPVs cause intraepithelial lesions that can progress to invasive cell carcinoma (*6*). Depending on the geographical region, ∼70% of human cervical cancers are associated with infections by high-risk HPV16 and HPV18 (*7*). Papillomaviruses contain eight or nine protein products, lack a DNA replication machinery, and thus rely on the host cell for the replication of the viral genomes. This is achieved by forcing host cells into the S phase, a strategy common to other DNA viruses such as SV40 and adenovirus (*3*). Parallel strategies have evolved in high-risk HPVs to target key cell cycle regulatory proteins. Following stochastic integration of HPV DNA into the host genome with the concomitant disruption of the E2 transcriptional regulator (*8*, *9*), it is the uncontrolled production of early proteins E6 and E7 which plays the main role in the development of cervical cancer (*5*, *6*, *10*). E6 and E7 promote the degradation of tumor suppressors p53 and pRb, respectively (*6*), and are necessary and sufficient for transformation (*11*).

E6 is a small protein (150 amino acids), in particular considering the growing list of described interacting partners. A useful classification of the so far described interacting partners of E6 shows four broad groups: (i) transcription factors, co-activators, and signal transducers, (ii) pro-apoptotic proteins, (iii) proteins involved in cell architecture, polarity, and adhesion, and (iv) DNA replication and repair factors (*12*). A recent comprehensive review of E6 activities related to malignant progression points out the difficulty of cataloguing all the oncoprotein targets that have been described (*2*). Since many related DNA tumor viruses are

† M.M.G.-A. and C.S. are recipients of Ph.D. scholarships from the University of Buenos Aires. G.P.G. is a Career Investigator from CONICET. This work was supported by ICGEB (CRP ARG0102) and ANPCyT (PICT 01-10944).

‡ Instituto Leloir and CONICET.

§ UBA.

10.1021/bi602457q CCC: $37.00
Published on Web 12/19/2006

implicated in cell transformation through parallel or equivalent pathways, a subset of targets was outlined, based on conservation of function across the different viruses reducing the number of possible targets, and many of them have not yet had biological significance demonstrated (*2*). Nevertheless, a growing consensus suggests that the main transforming properties of E6 are related to p53 degradation on one hand and its ability to promote malignant progression by targeting PDZ domain-containing proteins which affect cell adhesion and polarity on the other (*13*). In addition, high-risk E6 is known to produce immortalization of primary human epithelial cells through the induction of telomerase at a transcriptional level (*5*, *14*).

A two-domain protein bearing two CXXC motifs each (*15*), E6 was described as associating with the HECT domain family of proteins (*16*). HPV16 and HPV18 E6 contain 14 and 12 cysteine residues, respectively, which hindered biophysical characterization and refolding methods for obtaining substantial and homogeneous amounts of recombinant protein. A recently determined structure of the C-terminal domain of a six-cysteine mutated form of HPV16 E6 was obtained by NMR and reveals a novel zinc binding fold (*17*).

Since E6 targets different proteins in the cell, a main goal is unequivocally linking its bona fide biological activities and mechanisms to their cellular distribution for the endogenous protein in HPV-transformed cells. High-risk transfected HPV E6 were reported to localize in the cytoplasmic perinuclear region (*18*), to be colocalized in the cytoplasm with p53 (*19*), to be colocalized in the nucleus and perinuclear region (*20*, *21*), and to be evenly distributed in the cytoplasm and the nucleus (*22*), depending on the cell line that is used, the high-risk HPV type, and the fusion protein at which antibodies were addressed (*21*). Different authors have assigned these contradictory results to "the poor reactivity" of the anti-E6 existing antibodies. Thus, E6 has been regarded as a protein that is expressed at very low levels in cells, and the endogenous oncoprotein has not been detected in transformed untransfected cells to date.

In this work, we show that recombinant high-risk HPV16 and HPV18 E6 readily fold into very stable soluble oligomers (E6SOs) that exhibit secondary and tertiary structure, cooperatively lost upon denaturation. Polyclonal antibodies produced against these allow a precise analysis of the cellular distribution of the oncoproteins in two prototypic HPV-transformed cell lines, HeLa and CaSki. We find a predominantly nuclear localization of the monomeric forms of E6 and a predominantly cytoplasmic localization for E6 species sharing the conformational epitopes found in the oligomeric immunogens. We discuss the localization of E6 in these cell lines in connection to the two most accepted carcinogenic mechanisms described for this protein: p53-mediated transformation and PDZ-mediated malignant progression.

EXPERIMENTAL PROCEDURES

Plasmids. pET15b-HPV18 E6 was kindly provided by C. Arrowsmith. The HPV16 E6 gene was amplified from the HPV16 genome and cloned into pGEM-T (Promega) with the following primers: Fw, 5′-GGAATTCCATATGCACCAAAAGAGAACT-3′; Back, 5′-CGGGATCCTTACAGCTGGGTTTC-3′. To eliminate an internal restriction site for NdeI in the E6 coding sequence, a silent mutation was introduced by inverse PCR (Fw, 5′-TACGCTGTATGTGATAAATG-3′; and Back, 5′-GGATTCCCATCTCTATATAC-3′) and subcloned into pETt15b (Novagene) at NdeI and BamHI sites. pT7 cDNA/p53 used for the degradation experiments was kindly provided by V. Gottifredi.

Expression and Purification of Recombinant HPV18 and HPV16 E6. E6 was cloned as a fusion protein with a six-His tag and expressed in the *Escherichia coli* BL21(DE3) strain. Cell cultures were grown in 4 L of LB medium at 37 °C containing 100 μg/mL ampicilin. The culture was induced with 0.5 mM IPTG at an OD of 0.6, and 150 μg/mL Rifampicin was added 2 h after induction. Cells were harvested by centrifugation after 18 h from induction and stored at −70 °C. The pellet was resuspended in buffer A [50 mM Tris-HCl (pH 7.5) and 10 mM 2-M], lysed by sonication, and centrifuged at 12 000 rpm. Inclusion bodies (IBs) were extensively washed in 4 M urea and buffer A, further resuspended in 6 M GdmCl, and finally diluted in buffer B [20 mM Tris-HCl (pH 7.5) and 6 M urea, to avoid using large quantities of GdmCl]. The sample was loaded in a chelating Sepharose fast flow column (Amersham Biosciences) loaded with $NiCl_2$ and eluted with a gradient of buffer containing 0 to 0.5 M imidazole. The refolding step was performed by dialyzing the fraction against buffer C [1 mM DTT, 20 mM sodium acetate (pH 5.0), and 5 μM $ZnSO_4$] overnight at 4 °C. To obtain monomeric E6, refolding was carried out in the absence of reductant for HPV16 E6 and by adding 5 μM $CdCl_2$ for HPV18 E6 in the dialysis. The refolded protein was concentrated on an AMICON filtration unit (Millipore) and subsequently subjected to gel filtration chromatography on a Biosil 250 column (Bio-Rad) for E6SOs or Superdex 75 (Amersham Pharmacia) for monomeric E6. Protein concentrations were determined by the Bradford colorimetric assay and the OD at 280 nm.

Because of pH restrictions, thrombin could not be used to cleave the His tag. Nonfused HPV18 E6 was obtained by chemical hydrolysis of the His-tagged form with CNBr (2 mg/mg of protein) in 6 M GdmCl and 1% HCl for 4 h, desalted, and reloaded in a chelating Sepharose fast flow column (Amersham Biosciences). Both proteins with or without the His tag form large oligomers, exhibit similar CD spectra, and behave similarly toward pH and salt concentration (see Figure 1 of the Supporting Information). Because of the low yields in production of nontagged proteins, the His-tagged forms were used throughout the work.

Spectroscopic Analysis. CD measurements were carried out on a Jasco J-810 spectropolarimeter (Jasco) employing a scan speed of 100 nm/min, a band-pass of 1 nm, and an average response time of 4 s. All spectra were an average of 10 scans. The temperature was kept at 25 °C using a Peltier-controlled sample compartment. Spectra of high-risk HPV E6 at 10 μM were registered on a 0.1 cm path length cell. Each sample of GdmCl for unfolding experiments was incubated for 4 h in 10 mM sodium acetate buffer (pH 5.0) before the measurement. Melting curves were monitored following the amplitude of the negative band at 222 nm as a function of temperature. For pH experiments, 20 mM sodium formiate (pH 2.5−4.2), sodium acetate (pH 4.5−6.0), or Tris-HCl (pH 6.8 and 7.5) was used.

Scattering was measured on an Aminco-Bowman spectrofluorimeter, setting excitation and emission at 360 nm with a 4 nm band-pass as a function of time during 120 s and collecting data every 5 s.

Size Exclusion Chromatography. Analytical size exclusion chromatography (SEC) experiments for E6SOs were carried out on a Biosil 250 column (Bio-Rad) equilibrated in 20 mM sodium acetate (pH 5.0) and 1.0 M GdmCl. Monomeric E6 filtration was carried out in a Superdex 75 column equilibrated with 20 mM sodium acetate buffer (pH 5.0) and 0.3 M GdmCl, and elution of the protein was detected at 225 (HPV18) and 280 nm (HPV16). The column was calibrated with the following standard proteins: BSA (67 kDa), ovalbumin (43 kDa), chymotrypsinogen A (25 kDa), and ribonuclease A (16.4 kDa) from the gel calibration kit (Amersham Pharmacia). The void volume (V_0) and total volume ($V_o + V_i$) were measured by loading blue dextran and acetone, respectively, at both GdmCl concentrations to exclude column compression.

Light Scattering. The weight-averaged M_w of E6SOs was determined on a Precision Detectors PD2010 light scattering instrument tandemly connected to a high-performance liquid chromatography system and an LKB 2142 differential refractometer. Two hundred microliters of HPV16 and HPV18 E6SOs (1 mg/mL approximately) were loaded on a Superose 6 column (Amersham Pharmacia) and eluted with 20 mM sodium acetate buffer, containing 1.0 M GdmCl. The 90° light scattering and refractive index signals of the eluting material were recorded on a personal computer and analyzed with the Discovery32 software supplied by Precision Detectors. The 90° light scattering detector was calibrated using bovine serum albumin ($M_w = 66.5$ kDa) as a standard. Prior to the injection into a size exclusion chromatography column (SEC), each sample was preincubated for 1−2 h at room temperature in the elution buffer.

Atomic Force Microscopy. For AFM imaging, protein E6 was diluted to 1 ng/μL in buffer containing 10 mM MES (pH 5.0) and 1 mM $MgCl_2$. Twenty microliters of the mix was deposited onto freshly cleaved muscovite mica. After 2−5 min, the sample was gently washed with 0.5 mL of Milli-Q water to remove molecules that were not firmly attached to the mica and blown dry with nitrogen. Tapping-mode AFM was performed using a Nanoscope III Multimode atomic force microscope (Digital Instruments, Veeco Metrology, Santa Barbara, CA) with a J type piezoelectric scanner with a maximal lateral range of 120 μm. Micro-fabricated silicon cantilevers 125 μm in length with a force constant of 40 N/m were used (NanoDevices, Veeco Metrology). The cantilever oscillation frequency was tuned to the resonance frequency of the cantilever (280−350 kHz). After a period of thermal relaxation of 15−30 min, initial engagement of the tip was achieved at scan size zero to minimize sample deformation and tip contamination. The images (512 × 512 pixels) were captured with a scan size between 0.5 and 3 μm at a scan rate of 1−2 scan lines/s. Images were processed by flattering using Nanoscope software (Digital Instruments) which was used to remove background noise. For the statistical analysis, the diameter was measured in the middle of the height of the cross section by measuring 50 individual oligomers and analyzed by using Origin version 5.0.

Antibodies. Plolyclonal anti-HPV E6 antibodies against highly purified E6SOs were raised in rabbits using standard procedures. Both sera exhibited high titer when tested for an indirect ELISA against its corresponding antigen; 0.25 μg of HPV16 or HPV18 E6SOs in 10 mM sodium acetate (pH 5.0) was used for coating PolySorp plates (Nunc, Rockville, Denmark) and blocked in 1% BSA TBS. Peroxidase-conjugated goat anti-rabbit secondary antibodies were obtained from DakoCytomation, and OPD was used as a substrate.

Immunofluorescence. HeLa, CaSki, and U2Os cells, obtained from American Type Culture Collection (Rockville, MD), were grown on 12 mm diameter glass coverslips (Marienfeld) to ~80% confluence in DMEM containing 10% fetal bovine serum, 20 units/mL penicilin, and 20 g/mL streptomycin at 37 °C under 5% CO_2. The cells were fixed with cold methanol for 10 min at −20 °C, blocked with 10% donkey normal serum in PBS containing 0.1% Triton X-100 for 30 min at room temperature, and subsequently washed and incubated with primary polyclonal antibodies (anti-E6 HPV18, 1:200; and anti-E6 HPV16, 1:100) for 2 h in blocking solution. The cells were treated with Cy3-Dye-labeled donkey anti-rabbit IgG (1:800, Jackson Immuno-Research) for 40 min. 6-Diamino-2-phenylindole (DAPI, 1:1000) was added for detection of the nuclei. The coverslips were mounted with Gelvatol. Control experiments were performed with preimmune serum instead of primary antibody, and the immune−adsorption experiment was carried out by preincubating the primary antibodies with 1 mg/mL of HPV16 and HPV18 E6SOs or monomeric forms in PBS for 1 h at room temperature. Images were obtained in an LSM 510 PASCAL confocal microscope (Carl Zeiss, Oberkochen, Germany).

In Vitro p53 Degradation Assays. The p53 gene was transcribed and translated in vitro using the TNT T7 Quick Coupled System (Promega), with L-[^{35}S]Met (Amersham Bioscience) and pT7 cDNA/p53 or pT7 cDNA/Luciferase as a control. The transcription−translation reaction was performed at 30 °C for 90 min following standard kit indications in a final volume of 10 μL. Aliquots (5 μL) of the translated p53 and 2 μL of Luciferase were mixed and incubated for 15 min with 0.5 μg/mL HPV16 E6 at room temperature when specified. For the actual degradation reaction, 10 μL of HeLa extract (1 mg/mL total protein) was added in buffer D [25 mM Hepes (pH 7.5), 1 mg/mL BSA, 2 mM ATP, 4 mM $MgCl_2$, 1 mM DTT, 0.11 μg/μL creatine kinase, and 10 mM P-creatine] instead of fresh reticulocyte lysate. Samples were incubated for 2 h at 30 °C and then mixed with SDS containing sample buffer at 90 °C for 10 min. For control experiments, HeLa extracts were incubated with 40 μM MG132 (Sigma) for proteasomal inhibition. The samples were analyzed by SDS−PAGE and phosphorimaging (STORM 840, Molecular Dynamics).

P53 Binding Experiments. In vitro-translated L-[^{35}S]Met-p53 was preincubated at 30 °C with 0.5 μg of HPV E6 in 1 mL of buffer containing 50 mM Tris-HCl (pH 7.5), 150 mM NaCl, 0.5% sodium deoxycholate, 1% NP40, 0.01% SDS, and 0.5 mM PMSF. After 1 h, serum anti-E6SOs (1:1000) was added and the mixture incubated at 30 °C for 45 min. For immunoprecipitation, a protein G−Sepharose suspension (Amersham Biosciences) previously equilibrated in binding buffer was added and the mixture incubated at room temperature with agitation for 30 min. After the sample had been washed several times with binding buffer, the resin was

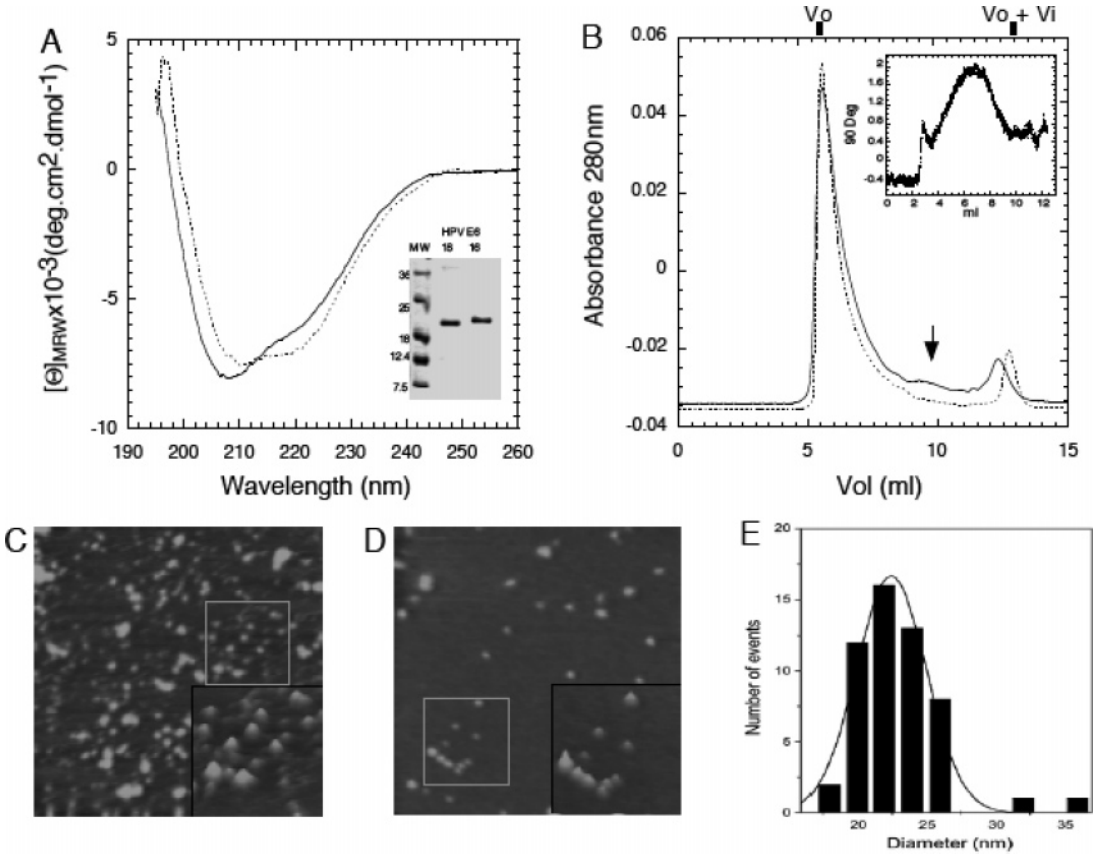

FIGURE 1: High-risk HPV18 and HPV16 E6 display differences in their secondary structure composition, and both form high-molecular mass oligomers in solution. **(**A) Far-UV CD spectra of wild-type high-risk HPV16 (—) and HPV18 (···). The inset shows SDS−PAGE of the purified proteins. (B) Size exclusion chromatography of HPV16 E6 (—) and HPV18 E6 (···). Both proteins exhibit hydrodynamic radii larger than that of a globular protein of 300 kDa and elute in the void volume (V_0) of the column. The inset shows the 90° light scattering refractive index signal of the eluting E6SOs from a Superose column. (C−E) Visualization of E6 oligomers by atomic force microscopy. Images in air of HPV16 (C) and HPV18 (D) E6SOs. For the top view images, the *xy* scale is 1 μm and the *z* scale is 0−10 nm. The inset shows magnifications of selected areas. (E) Statistical distribution for HPV18 E6SOs measured diameters. The data have been fitted to a Gaussian distribution (—), and the mean diameter is 22.4 nm with a standard deviation of 2.5 nm. The thin distribution arises principally from structural homogeneity within the oligomers.

cracked in buffer containing SDS at 100 °C and finally loaded on a SDS−PAGE gel. The experiment was developed by phosphorimaging.

RESULTS

HPV16 and HPV18 E6 Fold into Large Soluble Oligomers. Wild-type high-risk HPV16 and HPV18 E6 were expressed, purified, and refolded to yield fully soluble forms that exhibit secondary structure typical of a folded protein, particularly one rich in α-helix (Figure 1A). HPV18 E6 exhibits an increased α-helical content with respect to HPV16, the basis of which could be the presence of residue P95 at α-helix H1 found in the solution structure of HPV16 E6 (*17*), which has a glycine residue in the HPV18 protein. When subjected to size exclusion chromatography, both proteins eluted as large oligomers in the void volume of the column, indicating molecular masses of more than 300 kDa, with no observable monomeric or otherwise low-molecular mass species (Figure 1B). Dynamic light scattering allowed us to determine molecular masses of 1.4 MDa for HPV16 and 1.18 MDa for HPV18 (Figure 1B, inset), indicating that the supramolecular structures are formed by at least 60 monomers.

To evaluate the actual morphology of the oligomers, we carried out atomic force microscopy analyses, and these showed spherical shapes (Figure 1C,D). Both proteins exhibit similar overall macromolecular structures, i.e., spheres of ∼20-25 nm, but HPV18 E6 (Figure 1D) appears to be more regular and homogeneous than HPV16 E6 and thus amenable to statistical analysis, yielding a mean diameter of 22.5 nm. HPV16 E6 (Figure 1C) appears to be more heterogeneous, presenting several clusters of oligomers and spheres of different sizes that hinder a statistical analysis. Despite these morphological differences, both proteins remain highly soluble under the pH conditions that were used, with HPV16 E6 presenting different oligomeric states that become more evident once placed on the mica. On the basis of these results, we named the species E6 spherical oligomers (E6SOs), in accordance with our previous notation for the E7 spherical oligomers (*23*).

As opposed to the E7 oligomers that exhibit repetitive β-sheet structure found in amyloid-type structures (*23*), the E6SOs do not bind congo red or thioflavin T, indicators of this type of structure (data not shown). pH analysis shows that while HPV16 E6 remains soluble throughout the pH range that was tested, HPV18 E6 aggregates to yield insoluble precipitates above pH 5.1 (Figure 2A), with an extremely sharp transition, within a 0.1 pH unit change, as the increased light scattering indicates. Both high-risk E6SOs are highly stable to thermal denaturation, where the spectra

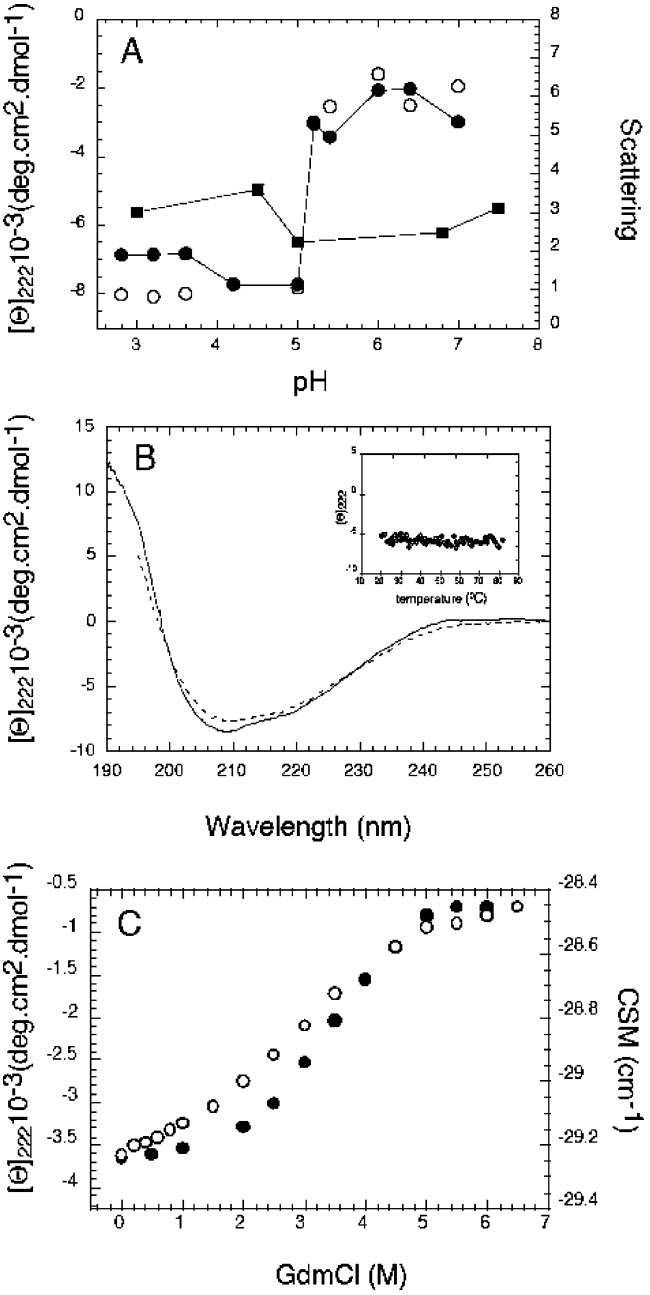

FIGURE 2: Biophysical characterization of E6SOs. (A) Molar ellipticity at 222 nm of E6 HPV16 (■) and HPV18 (●) as a function of pH. HPV18 E6 was also followed by light scattering at 360 nm (○). (B) Stability of E6SOs to heat denaturation analyzed by far-UV CD. Spectra of HPV18 E6 at 20 (—) and 80 °C (···). The inset shows the molar ellipticity of HPV16 E6 at 222 nm as a function of temperature. (C) Cooperative unfolding of HPV16 E6 by GdmHCl, followed by molar ellipticity at 222 nm (●) or by its center of spectral mass (○).

of both proteins at 25 and 80 °C are superimposable (Figure 2B shows HPV18 E6) and no change in the hydrodynamic volume was observed after heating (not shown). Gradual heating of HPV16 E6 produces no change in the secondary structure up to 80 °C (Figure 2B, inset). An unfolding experiment with the E6SOs was carried out to further test its stability and the presence of cooperativity, indicative of compact and discrete ordered structures. Figure 2C shows the chemical unfolding of the transition of HPV16 E6SOs that indeed displays a clear cooperative loss of secondary structure, as the change in molar ellipticity indicates. The fluorescence spectrum of HPV16 E6SOs shows a buried tryptophan residue (Figure 2A of the Supporting Information) that can be used to follow changes in tertiary structure indicated by the gradual exposure of the Trp residue to the solvent. The change in the fluorescence center of spectral mass changes cooperatively but precedes slightly the ellipticity change, indicating that the loss of tertiary and secondary structure does not take place in parallel. Analysis of the near-UV CD shows that the weak negative band of HPV16 E6 disappears at 6.0 M GdmCl (Figure 2B of the Supporting Information). In any case, the cooperativity suggests a rather compact nature of the oligomers. The fact that the oligomeric species are highly stable, cooperative, and discrete prompted us to use them for obtaining antibodies for further immunological analysis in cells.

Antibodies against E6SOs Readily Detect Endogenous E6 in HPV-Transformed Cell Lines. The oligomers allowed us to obtain high-titer polyclonal sera against both proteins (Figure 3 of the Supporting Information), and our first goal was to investigate the presence of E6 in naturally transformed cell lines. The CaSki cell line contains 600 copies of an HPV16 genome integrated per cell, while HeLa cells contain a low copy number of HPV18 genomes with weak expression of p53 (*24*). Polyclonal antibodies against HPV16 E6SOs detect E6 in CaSki cells and show a uniform distribution of the oncoprotein in nuclei and cytoplasm in all fields that are inspected (Figure 3B,C). Using the preimmune serum in the same dilution shows no label (Figure 3D), and omission of the first antibody yields identical results (not shown). As an additional control, the anti-HPV16 E6 polyclonal serum was pre-adsorbed with a large excess of pure HPV16 E6SOs, and no label was observed (Figure 3E). An identical situation was observed in HeLa cells with anti-HPV18 E6SOs antibodies (Figure 3G−J). The cellular distribution was confirmed by a *z* stack analysis of the different image layers for both cells (see Figure 4 of the Supporting Information). To rule out nonspecific labeling, human osteosarcoma cells (U2OS) were tested for both sera [anti-HPV16 E6 (Figure 3A) and anti-HPV18 E6 (Figure 3F)] in the immunofluorescence assay with no detectable signal.

Differential Nuclear Localization of the Monomeric Forms of E6. By modifying the refolding conditions, we could produce monomeric forms of E6 from both high-risk types (see Experimental Procedures). The monomeric forms resemble the E6SOs in terms of secondary structure with evidence of α-helical content (see Figure 2C of the Supporting Information). When subjected to SEC, combined with dynamic light scattering analysis (DLS), they both exhibited a molecular mass that agrees with that expected from their amino acid sequences. Figure 4A shows the elution profile of the HPV16 E6 monomer, and its molecular mass, according to DLS, was 23.1 kDa. The calculated stock radius is 24.7 Å; however, using algorithms that relate molecular mass with hydrodynamic volume (*25*), the expected radius for a globular protein of the size of E6 from a SEC experiment (21.3 kDa) is effectively 21.3 Å. This 16% discrepancy suggests that the conformation of the monomeric conformer resembles a molten globule-like structure, normally between 10 and 20% larger than the globular compact shape (*25*).

Degradation assays in the presence or absence of the proteasome inhibitor MG132 show that monomeric E6 from

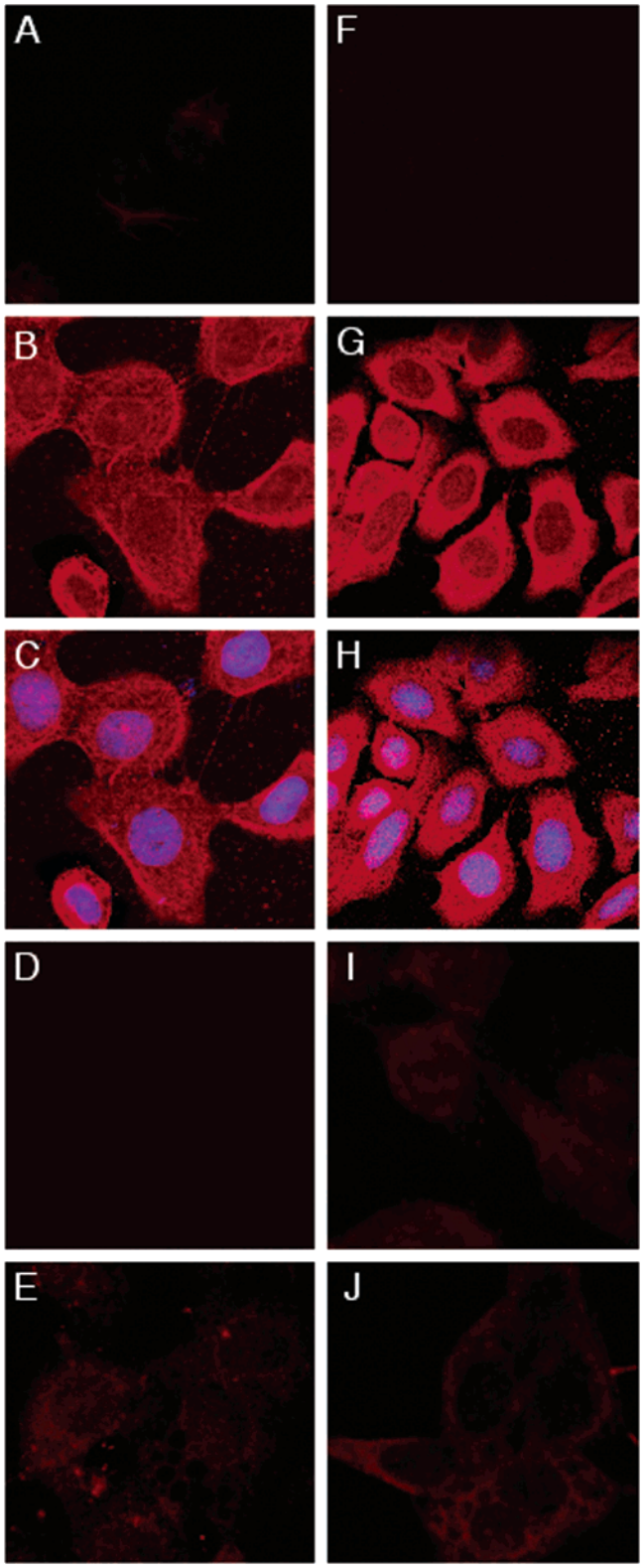

FIGURE 3: Indirect immunofluorescence analysis. U2OS cells were tested with anti-HPV16 E6 (A) and anti-HPV18 E6 serum (F) as controls for nonspecific labeling of cellular components. The left column corresponds to labeling with anti-HPV 16 E6 and the right column to anti-HPV18 E6 polyclonal serum. (B) Immunolabeling of CaSKi cells with polyclonal anti-HPV16 E6SOs antibodies. (C) Merge image with DAPI. (D) Image using preimmune serum as the first antibody and (E) after neutralizing the anti-HPV16 serum with 1 mg/mL HPV16 E6SOs. (G−J) Same sequence of experiments as in panels B−E, but with HeLa cells and anti-HPV18 E6 polyclonal seurm as the first antibody.

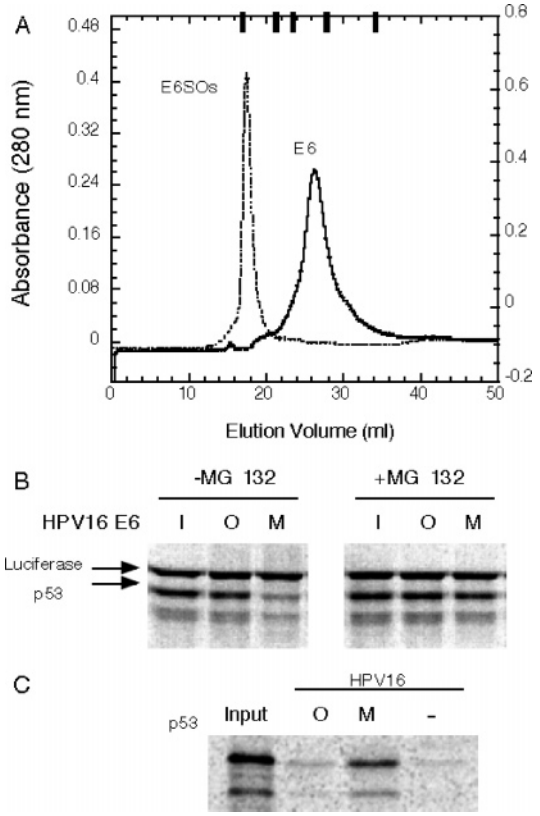

FIGURE 4: In vitro degradation of p53 by E6 conformers. (A) SEC of HPV16 monomeric E6 and E6SOs, with the molecular mass markers described in Experimental Procedures indicated with bars. (B) p53 degradation assay. For SDS−PAGE, [^{35}S]Met-p53 and [^{35}S]-Met-luciferase proteins were incubated with HPV16 monomeric E6 (M), E6SOs (O), or mock (no E6 added, I), in the presence (right) or absence (left) of proteasome inhibitor MG132. (C) p53 binding assay in which [^{35}S]Met-p53 was immunoprecipitated with anti-HPV16 E6 in the presence of E6 monomeric form (M) or E6SOs (O). No E6 added in I as control.

HPV16 is active in promoting the proteasomal-mediated degradation of p53, and the E6SOs are virtually inactive under the same assay conditions (Figure 4B). To evaluate whether the lack of p53 degradation by E6SOs correlated with binding to p53, we carried out immunoprecipitation experiments. In vitro-translated p53 was treated with either monomeric or oligomeric E6 and "pulled down" using our anti-E6 polyclonal antibodies and protein G-Sepharose. The binding results show that the lack of p53 degradation activity correlates with the lack of binding of the tumor suppressor, most likely forming ternary complexes with E6AP, where E6SOs binds p53 very poorly compared to monomeric HPV16 E6 under the same conditions (Figure 4C). Similar results were obtained for HPV18 E6 (not shown).

Finally, we wanted to evaluate whether the monomeric and oligomeric species, or whatever structures share epitopes with them, were distinguishable in cells. To address this question, we pre-adsorbed the anti-E6 polyclonal antibodies of both strains with an excess of the respective monomeric species (1 mg/mL conformationaly pure protein), to ensure antibody saturation of populations recognizing monomers only. The immunofluoresence of CaSki and HeLa cell lines with sera pre-adsorbed with purified monomeric protein from each strain shows that the nuclei of both cells are completely devoid of fluorescent label (Figure 5A−D). These images should be contrasted with those in Figure 3 where E6 staining

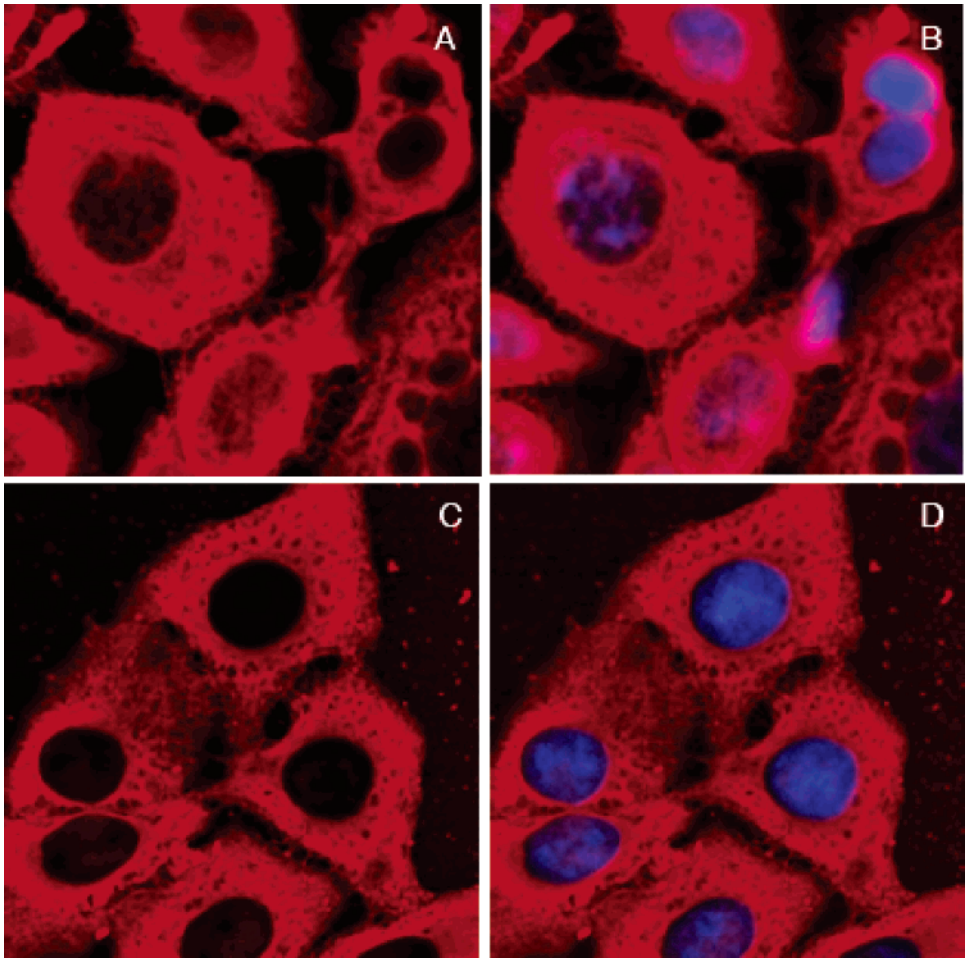

FIGURE 5: Nuclear localization of monomeric forms of E6. Indirect immunofluorescence analysis of E6 detected in CaSKi (A) and HeLa (C) cells previously adsorbed with HPV16 and HPV18 monomeric E6. Polyclonal antibodies anti-E6SOs detect the protein distributed in the cytoplasm, but the nucleus has been depleted of label. Panels B and C show panels A and D merged with DAPI. A *z* stack analysis of the images showing the lack of nuclear label throughout the different layers is shown in the Supporting Information.

is both cytoplasmic and nuclear. This clear-cut result indicates that species of both high-risk E6 that share epitopes with monomeric forms are preferentially localized in the nucleus and no oligomeric forms access or accumulate in that compartment. As shown in panels C and G of Figure 3, preneutralization of the sera with the same amount of E6SOs leads to the complete disappearance of the label, indicating that most of the clonal lines represented in the sera recognize the oligomer and that some of the epitopes are shared with the monomers, but not the other way around.

DISCUSSION

HPV-transforming proteins have been described to cause various effects on cells depending largely on cell types, protein constructs, fusions, expression levels, and the methods and reagents that are used. Among those effects, a subset is clearly relevant on the basis of conserved functions across other tumor viruses (*2*). Fundamental questions remain, however, such as the extent to which the endogenous oncoproteins are expressed in infected or transformed cells, and the cellular distribution provides clues about their precise mechanisms. In this work, we describe that E6 readily forms stable oligomers in solution and use them to address the simple question of the level of endogenous expression of E6 from the two high-risk HPV species that account for 70% of the cervical cancers worldwide, in prototypic transformed cell lines of each viral type.

The first issue is which are the most stable forms of recombinant E6 proteins that can be produced. We found that both HPV16 and HPV18 E6 assemble into large spherical oligomers 22−25 nm in diameter and 1.2−1.4 MDa in molecular mass, and we named them E6SOs. These structures are formed spontaneously and are very stable to temperature denaturation. The cooperativity of the chemical denaturation indicates compact and discrete structures, which is also evident from atomic force microscopy images and chromatography experiments. The secondary structure content of the proteins includes substantial α-helix, in line with the recently determined solution structure of a six-Cys mutant of HPV16, as well as the fact that a proline residue in helix H1 of HPV16 anticipates less helical content than proteins from other strains, including HPV18. One important biochemical difference between these oligomers is that HPV18 E6 is extremely sensitive to a pH-dependent aggregation, which takes place from pH 5.0 to 5.1. It would not be surprising if the conditions in different compartments can cause these types of effects, where the exact absolute pH can be influenced by other cellular factors. Oligomeric species were reported for fused forms of E6 but were described as being not soluble and not homogeneous or were not analyzed in detail (*26*, *27*).

Although common origins via gene duplication have been proposed for E6 and E7 (*28*) and both appear to form large spherical oligomers, E7SOs have repetitive β-sheet structures similar to those found in amyloid conformations (*23*), different from the α-helical structure in E6SOs. By modifying the refolding conditions, we could obtain E6 monomers, albeit not as stable as the oligomers, which provide another conformer for investigating possible equilibria that can exist under physiological conditions. In fact, only monomeric forms of a six-Cys HPV16 E6 mutated protein or a protein fused to the B1 subdomain of protein G were described (*17*, *29*).

Once we identified the most stable conformers that could be obtained for recombinant high-risk E6 proteins, we moved onto investigating their presence and distribution within HPV-transformed cell lines. Using the antibodies raised against E6SOs, we found that endogenous E6 is effectively expressed at high levels in CaSki and HeLa cell lines. Irrespective of discriminating which conformer is present, this result contrasts with previous references to low levels of endogenous oncoprotein. The immunofluorescence images show both high-risk E6 proteins distributed uniformly in the cell and cytoplasm. Depletion of the polyclonal sera with monomeric species of E6 indicates that the monomers are located preferentially in the nucleus, while E6SOs, or the structures sharing epitopes with these, are located evenly distributed in the cytoplasm but do not have access to the nucleus. It is surprising that epitopes from the E6SOs are not present in the monomeric forms; this could be explained by the fact that oligomerization involves a substantial conformational change, suggesting that the remaining epitopes in the oligomers are conformational rather than linear. Perhaps this is one reason why to date no strong signal of E6 could be detected using monoclonal antibodies. The fact that almost identical results are obtained for the two main high-risk types in two cell lines using similarly obtained antibodies in parallel experiments is highly significant.

The nuclear localization of the monomeric conformers of endogenous E6 in transformed cell lines indicates a close correlation with its anti-p53 effect, the first and best described tumor suppressor target for this viral oncoprotein. Only the monomeric forms of E6 can promote p53 degradation in vitro, and the localization of p53 is known to be primarily nuclear in these transformed cells (*30*, *31*). Since high-risk E6 was reported to interact with at least six PDZ domain proteins (*2*), and these are mostly cytoplasmic, the correlation with the targets that are disrupted is not unexpected. These proteins are required for the maintenance of the cell architecture and adherence in general, as well as inhibitors of cell proliferation, and therefore, they are thought to be main targets for high-risk E6s. A recent report shows that while HPV18 E6 is more efficient in targeting hDlg, the HPV16 counterpart is more efficient for assisting hScrib degradation (*32*). Both proteins are believed to participate in a complex that modulates cell polarity (*33*), and the two viral strains would have a complementary effect on both hDLG and Scrib (*32*).

Figure 6 shows a model compatible with the results we present in this work. After being synthesized, E6 can have multiple destinations. It may fold as an independent monomer and translocate to the nucleus, where it exerts its anti-p53 effect. As we now show, it can remain in the cytoplasm as possible large oligomeric species. However, we believe that the "oligomeric E6" forms refer not only to homo-oligomers such as the ones we describe in vitro but also to hetero-oligomers with other proteins. These forms could likely involve multimolecular complexes of E6 with other cytosolic proteins such as PDZ domain proteins. In speculative terms, we believe that the building blocks of all homo- or hetero-oligomeric complexes will be monomeric species of E6, which so far appear to have a flexible extended and molten globule-like behavior, unikely to stay unbound to targets for long periods without the risk of a fast turnover. E6SOs, which are complexes containing only E6, may exist as pools when the concentration exceeds the capacity of interaction or nuclear translocation.

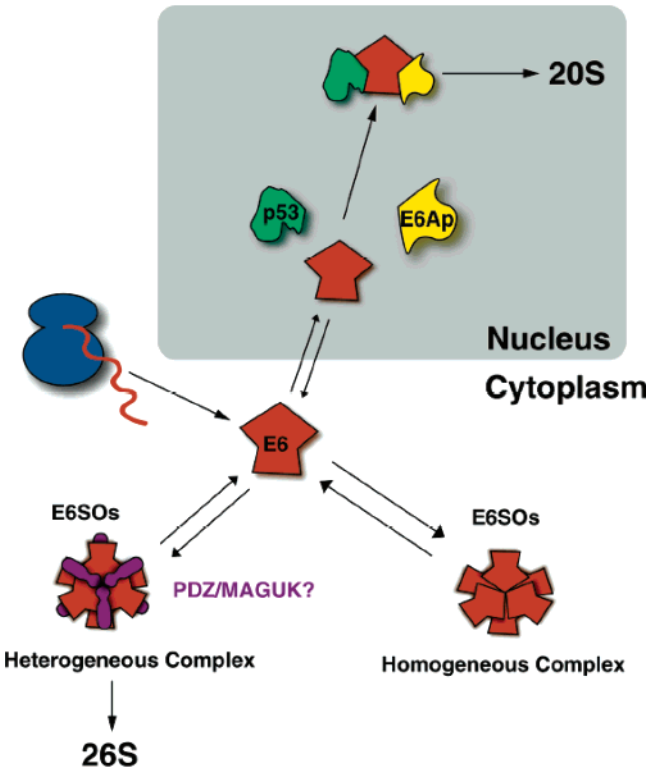

FIGURE 6: Model for the possible cellular distribution of endogenous high-risk E6 in cells (see the Discussion).

Despite being a small protein, E6 has diverse ways of participating in promotion and progression of cancer in epithelial cells and can hardly be limited to one specific effect or one target. This can be partly because of a structural plasticity and the idea that it exposes hydrophobic surfaces as well as charged regions to the solvent, but it certainly relates to the existence of conformational equilibria, which provide further ways of interfering with normal cell functioning. Among all the targets that have been described, the most crucial ones will be those participating in delicate regulatory functions of cell cycle control, cell polarity, or chromosome length in the case of telomerase (*5*). Any existing equilibria will be very complex and influenced by differentiation stage and stress. Future efforts should be directed into dissecting the biochemical species of endogenous E6 within the cells, and the most stable complexes that these form with the target proteins using highly specific antibodies, microscopic techniques, and proteomic approaches.

ACKNOWLEDGMENT

We thank Kevin Gaston and Eduardo Castaño for helpful comments and Rodolfo Tarelli for the assistance with microscopy images.

SUPPORTING INFORMATION AVAILABLE

High-risk HPV18 E6 six-His and nonfusion proteins displaying similar secondary structures (Figure 1), conformational analyses of HPV16 E6 (Figure 2), high-titer antibodies using E6SOs as an antigen (Figure 3), and optical sections from the immunofluorescence detection of E6 conformers in CaSki cells (Figure 4). This material is available free of charge via the Internet at http://pubs.acs.org.

REFERENCES

1. Lowy, D. R., and Howley, P. M. (2001) in *Fields Virology* (Fields, B. N., Howley, P. M., Griffin, D. E., Lamb, R. A., Martin, M. A., Roizman, B., Straus, S. E., and Knipe, D. M., Eds.) pp 2213−2219, Lippincott Williams and Wilkins, Philadelphia.
2. Thomas, M., Pim, D., and Banks, L. (2006) in *Papillomavirus Research* (Campo, M. S., Ed.) pp 115−131, Caister Academic Press, Wymondham, Norfolk, U.K.
3. Helt, A. M., and Galloway, D. A. (2003) Mechanisms by which DNA tumor virus oncoproteins target the Rb family of pocket proteins, *Carcinogenesis 24*, 159−169.
4. Zambetti, G. P. (2005) in *Protein Reviews* (Atassi, M. Z., Ed.) pp 1−23, Springer Science, New York.
5. Munger, K., Baldwin, A., Edwards, K. M., Hayakawa, H., Nguyen, C. L., Owens, M., Grace, M., and Huh, K. (2004) Mechanisms of human papillomavirus-induced oncogenesis, *J. Virol. 78*, 11451−11460.
6. Munger, K., and Howley, P. M. (2002) Human papillomavirus immortalization and transformation functions, *Virus Res. 89*, 213−228.
7. Durst, M., Gissmann, L., Ikenberg, H., and zur Hausen, H. (1983) A papillomavirus DNA from a cervical carcinoma and its prevalence in cancer biopsy samples from different geographic regions, *Proc. Natl. Acad. Sci. U.S.A. 80*, 3812−3815.
8. Yang, Y. C., Spalholz, B. A., Rabson, M. S., and Howley, P. M. (1985) Dissociation of transforming and trans-activation functions for bovine papillomavirus type 1, *Nature 318*, 575−577.
9. Soeda, E., Ferran, M. C., Baker, C. C., and McBride, A. A. (2006) Repression of HPV16 early region transcription by the E2 protein, *Virology* (in press).
10. Mantovani, F., and Banks, L. (2001) The human papillomavirus E6 protein and its contribution to malignant progression, *Oncogene 20*, 7874−7887.
11. Munger, K., Phelps, W. C., Bubb, V., Howley, P. M., and Schlegel, R. (1989) The E6 and E7 genes of the human papillomavirus type 16 together are necessary and sufficient for transformation of primary human keratinocytes, *J. Virol. 63*, 4417−4421.
12. Syrjänen, S. (2005) *HPV Today*, pp 8−10, BYPASS Ediciones, Madrid.
13. Simonson, S. J., Difilippantonio, M. J., and Lambert, P. F. (2005) Two distinct activities contribute to human papillomavirus 16 E6's oncogenic potential, *Cancer Res. 65*, 8266−8273.
14. Kiyono, T., Foster, S. A., Koop, J. I., McDougall, J. K., Galloway, D. A., and Klingelhutz, A. J. (1998) Both Rb/p16INK4a inactivation and telomerase activity are required to immortalize human epithelial cells, *Nature 396*, 84−88.
15. Barbosa, M. S., Lowy, D. R., and Schiller, J. T. (1989) Papillomavirus polypeptides E6 and E7 are zinc-binding proteins, *J. Virol. 63*, 1404−1407.
16. Huibregtse, J. M., Scheffner, M., Beaudenon, S., and Howley, P. M. (1995) A family of proteins structurally and functionally related to the E6-AP ubiquitin-protein ligase, *Proc. Natl. Acad. Sci. U.S.A. 92*, 5249.
17. Nomine, Y., Masson, M., Charbonnier, S., Zanier, K., Ristriani, T., Deryckere, F., Sibler, A. P., Desplancq, D., Atkinson, R. A., Weiss, E., Orfanoudakis, G., Kieffer, B., and Trave, G. (2006) Structural and functional analysis of E6 oncoprotein: Insights inthe molecular pathways of human papillomavirus-mediated pathogenesis, *Mol. Cell 21*, 665−678.
18. Daniels, P. R., Sanders, C. M., and Maitland, N. J. (1998) Characterization of the interactions of human papillomavirus type 16 E6 with p53 and E6-associated protein in insect and human cells, *J. Gen. Virol. 79* (Part 3), 489−499.
19. Liang, X. H., Volkmann, M., Klein, R., Herman, B., and Lockett, S. J. (1993) Co-localization of the tumor-suppressor protein p53 and human papillomavirus E6 protein in human cervical carcinoma cell lines, *Oncogene 8*, 2645−2652.
20. Kanda, T., Watanabe, S., Zanma, S., Sato, H., Furuno, A., and Yoshiike, K. (1991) Human papillomavirus type 16 E6 proteins with glycine substitution for cysteine in the metal-binding motif, *Virology 185*, 536−543.
21. Masson, M., Hindelang, C., Sibler, A. P., Schwalbach, G., Trave, G., and Weiss, E. (2003) Preferential nuclear localization of the human papillomavirus type 16 E6 oncoprotein in cervical carcinoma cells, *J. Gen. Virol. 84*, 2099−2104.
22. Guccione, E., Massimi, P., Bernat, A., and Banks, L. (2002) Comparative analysis of the intracellular location of the high- and low-risk human papillomavirus oncoproteins, *Virology 293*, 20−25.
23. Alonso, L. G., Garcia-Alai, M. M., Smal, C., Centeno, J. M., Iacono, R., Castano, E., Gualfetti, P., and de Prat-Gay, G. (2004) The HPV16 E7 viral oncoprotein self-assembles into defined spherical oligomers, *Biochemistry 43*, 3310−3317.
24. Schwarz, E., Freese, U. K., Gissmann, L., Mayer, W., Roggenbuck, B., Stremlau, A., and zur Hausen, H. (1985) Structure and transcription of human papillomavirus sequences in cervical carcinoma cells, *Nature 314*, 111−114.
25. Uversky, V. N. (2002) Natively unfolded proteins: A point where biology waits for physics, *Protein Sci. 11*, 739−756.
26. Nomine, Y., Ristriani, T., Laurent, C., Lefevre, J. F., Weiss, E., and Trave, G. (2001) Formation of soluble inclusion bodies by hpv e6 oncoprotein fused to maltose-binding protein, *Protein Expression Purif. 23*, 22−32.
27. Nomine, Y., Ristriani, T., Laurent, C., Lefevre, J. F., Weiss, E., and Trave, G. (2001) A strategy for optimizing the monodispersity of fusion proteins: Application to purification of recombinant HPV E6 oncoprotein, *Protein Eng. 14*, 297−305.
28. Cole, S. T., and Danos, O. (1987) Nucleotide sequence and comparative analysis of the human papillomavirus type 18 genome. Phylogeny of papillomaviruses and repeated structure of the E6 and E7 gene products, *J. Mol. Biol. 193*, 599−608.
29. Degenkolbe, R., Gilligan, P., Gupta, S., and Bernard, H. U. (2003) Chelating agents stabilize the monomeric state of the zinc binding human papillomavirus 16 E6 oncoprotein, *Biochemistry 42*, 3868−3873.
30. Dippold, W. G., Jay, G., DeLeo, A. B., Khoury, G., and Old, L. J. (1981) p53 transformation-related protein: Detection by monoclonal antibody in mouse and human cells, *Proc. Natl. Acad. Sci. U.S.A. 78*, 1695−1699.
31. Rotter, V., Abutbul, H., and Wolf, D. (1983) The presence of p53 transformation-related protein in Ab-MuLV transformed cells is required for their development into lethal tumors in mice, *Int. J. Cancer 31*, 315−320.
32. Thomas, M., Massimi, P., Navarro, C., Borg, J. P., and Banks, L. (2005) The hScrib/Dlg apico-basal control complex is differentially targeted by HPV-16 and HPV-18 E6 proteins, *Oncogene 24*, 6222−6230.
33. Woods, D. F., Wu, J. W., and Bryant, P. J. (1997) Localization of proteins to the apico-lateral junctions of *Drosophila epithelia*, *Dev. Genet. 20*, 111−118.

BI602457Q